Acta Crystallographica Section B
Structural Science
ISSN 0108-7681

Structures of six industrial benzimidazolone pigments from laboratory powder diffraction data

Jacco van de Streek,[a]‡ Jürgen Brüning,[a] Svetlana N. Ivashevskaya,[a,b] Martin Ermrich,[c] Erich F. Paulus,[d] Michael Bolte[a] and Martin U. Schmidt[a]*

[a]Institute of Inorganic and Analytical Chemistry, Goethe University, Max-von-Laue-Strasse 7, D-60438 Frankfurt am Main, Germany, [b]Institute of Geology, Karelian Research Centre, Russian Academy of Sciences, Pushkinskaya, 11, 185910 Petrozavodsk, Russia, [c]Röntgenlabor Dr Ermrich, Am Kandelborn 7, D-64354 Reinheim, Germany, and [d]Institute for Geosciences, Goethe University, Altenhöferallee 1, D-60438 Frankfurt am Main, Germany

‡ Current address: Avant-garde Materials Simulation, Merzhauserstrasse 177, D-79100 Freiburg i. Br., Germany.

Correspondence e-mail: m.schmidt@chemie.uni-frankfurt.de

Received 15 August 2008
Accepted 8 December 2008

The crystal structures of six industrially produced benzimidazolone pigments [Pigment Orange 36 (β phase), Pigment Orange 62, Pigment Yellow 151, Pigment Yellow 154 (α phase), Pigment Yellow 181 (β phase) and Pigment Yellow 194] were determined from laboratory X-ray powder diffraction data by means of real-space methods using the programs *DASH* and *MRIA*, respectively. Subsequent Rietveld refinements were carried out with *TOPAS*. The crystal phases correspond to those produced industrially. Additionally, the crystal structures of the non-commercial compound 'BIRZIL' (a chloro derivative of Pigment Yellow 194) and of a dimethylsulfoxide solvate of Pigment Yellow 154 were determined by single-crystal structure analyses. All eight crystal structures are different; the six industrial pigments even exhibit five different hydrogen-bond topologies. Apparently, the good application properties of the benzimidazolone pigments are not the result of one specific hydrogen-bonding pattern, but are the result of a combination of efficient molecular packing and strong intermolecular hydrogen bonds.

1. Introduction

Benzimidazolone pigments are organic 'azo' pigments containing a benzimidazolone moiety (see Fig. 1*a*). The pigments investigated here show yellow to orange colours and are produced industrially on a large scale (Herbst & Hunger, 2004; Metz & Morgenroth, 2002). Exactly one century ago, in 1909, the company Meister, Lucius & Brüning in Frankfurt am Main, Germany (later Farbwerke Hoechst AG, now Clariant GmbH), patented the 'Hansa®' yellow pigments (Fig. 1*b*) as one of the first classes of metal-free organic pigments. Hansa yellow pigments are widely used in lacquers and coatings, because they show good hiding power, excellent light fastness (photostability) and very good weather fastness (*i.e.* they do not fade). However, Hansa yellow pigments have one important drawback, which limits their field of application: they are to a small extent soluble in some organic solvents, and they are not completely insoluble in polymers either, resulting in migration. This problem was solved by chemically modifying the Hansa pigments: with the addition of a —NH—CO—NH— fragment, so-called 'benzimidazolone' pigments (Fig. 1*a*) were produced. They proved to be practically insoluble in all solvents and in all application media (Dietz & Schilling, 1963; Schilling & Dietz, 1964). The excellent light and weather fastness is unaffected, and therefore benzimidazolone pigments are widely used, especially for the colouration of polymers. The crystallite sizes are typically between 50 and 500 nm. In the polymers the pigments are not dissolved but finely dispersed, the crystal structures and properties being maintained in the final product. Hence, the differences in

properties between Hansa yellow and benzimidazolone pigments should be sought in the crystal structures of these pigments, and elucidating their crystal structures would therefore be a good starting point for understanding the more favourable properties of the benzimidazolone pigments compared with the Hansa pigments. Solving the crystal structures of organic pigments is not just an academic exercise: the majority of organic pigments are polymorphic, and the polymorphic form determines the colouristic properties. For example, in the mid-1990s, during the industrial production of the β polymorph of Pigment Orange 72 (P.O. 72, see Table 1), several tons of the γ polymorph (or mixtures of the β and the γ polymorph) were accidentally produced. Whereas the desired β phase is orange, the γ phase that was produced is brown, a colour that can be produced much more cheaply by *e.g.* mixing iron oxides with carbon black; as a consequence, the product could not be sold at a reasonable price. A transformation from the brown γ phase to the orange β phase requires rather harsh conditions, *e.g.* heating in melts of benzoic acid or β-naphthol, which is not economically feasible either. In the end, the brown γ polymorph had to be sold at a loss.

The solubility of the Hansa pigments makes it relatively easy to grow single crystals, and the Cambridge Structural Database (CSD; Allen, 2002) contains 25 unique crystal structures of Hansa pigments with atomic coordinates. Owing to the poor solubility of all benzimidazolone pigments in almost all solvents, *e.g.* alcohols, esters, ethers, acids and aromatic hydrocarbons, all attempts to grow single crystals from solution have so far failed; melting or sublimation is not possible either. [In our attempts to grow single crystals of these compounds, we did manage to dissolve Pigment Yellow 154 (P.Y. 154) in dimethylsulfoxide (DMSO) at 423 K and indeed single crystals of good quality could be grown – which turned out to be the DMSO solvate.] As a result, crystal structure determination from single-crystal data has thus far not been possible for any commercial yellow or orange benzimidazolone pigment. This is illustrated very well by the results we obtained when searching the CSD for the fragment shown in Fig. 1(*a*), which all commercial yellow mono-'azo'-benzimidazolone pigments have in common: in the entire CSD, only a single entry (CSD reference code BIRZIL; Hunger *et al.*, 1982) was found, without atomic coordinates. Furthermore, BIRZIL is only a derivative of a commercial pigment (chloro derivative of P.Y. 194), and BIRZIL itself is not of commercial interest. In other words, the insolubility of commercial benzimidazolone pigments has thus far prevented determination of any of their crystal structures, and no atomic coordinates of any such crystal structure have ever been published. (For red benzimidazolone pigments, which are based on β-naphthol as the coupling component, there is only one published crystal structure; Paulus, 1982.) In the current paper we will report the crystal structures of six commercially important benzimidazolone pigments: β-P.O. 36, P.O. 62, P.Y. 151, α-P.Y. 154, β-P.Y. 181 and P.Y. 194 (see Table 1). Since single crystals of the pure commercial products could not be grown, we had to determine these six crystal structures from X-ray powder diffraction data. Additionally, we report here the missing atomic coordinates of the crystal structure from the 1982 paper by Hunger *et al.* (CSD reference code BIRZIL). We also include the crystal structures of two solvates (β-P.Y. 154 and θ-P.Y. 181).

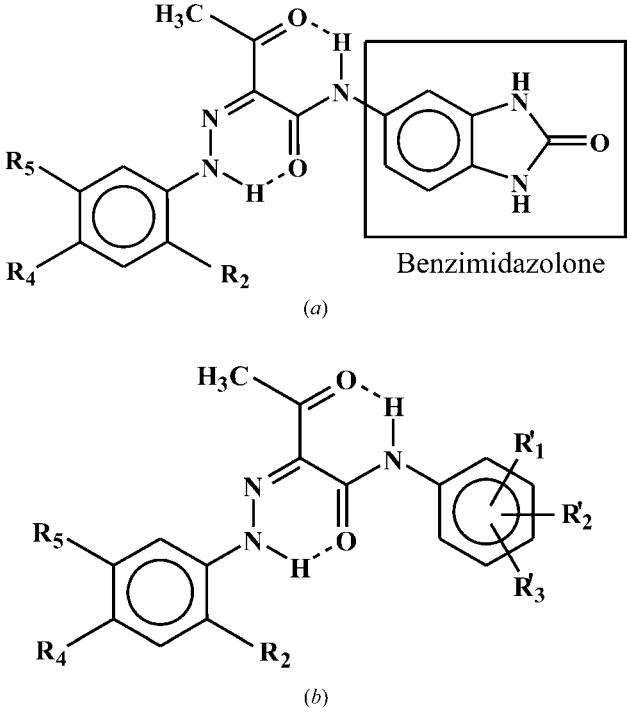

Figure 1
The structural formulae of (*a*) the benzimidazolone pigments and (*b*) the Hansa yellow pigments. For R_2, R_4 and R_5 see Table 1. R'_1, R'_2, R'_3 = —H, —Cl, —OCH_3, —CH_3 *etc*.

Table 1
The functional groups of the eight pigments discussed in this paper.

P.O. = Pigment Orange; P.Y. = Pigment Yellow; P.O. 72 =

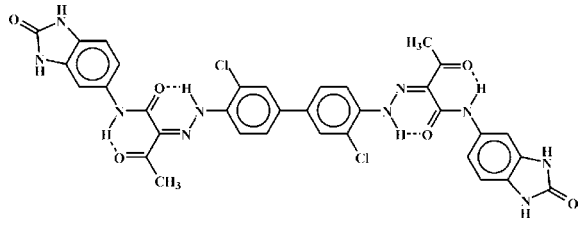

Pigment	R_2	R_4	R_5
P.O. 36	—NO_2	—Cl	—H
P.O. 62	—H	—NO_2	—H
P.Y. 151	—COOH	—H	—H
P.Y. 154	—CF_3	—H	—H
P.Y. 181	—H	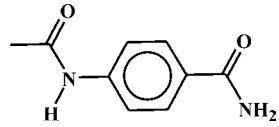	—H
P.Y. 194	—OCH_3	—H	—H
BIRZIL	—OCH_3	—H	—Cl
P.O. 72	—Cl	Inversion centre	—H

1.1. Synthesis, properties and polymorphism of the pigments

Benzimidazolone pigments (Herbst & Hunger, 2004; Metz & Morgenroth, 2002) are industrially synthesized by an azo coupling, as shown in Fig. 2. The syntheses are carried out in water and the pigments precipitate as a fine powder with crystal sizes far below 100 nm. In order to improve the dispersability and the opacity, most pigments are heated in solvents or water to 373–423 K to obtain particle sizes of up to 500 nm. In some cases (*e.g.* P.O. 36) the polymorphic form changes during this treatment. Originally, azo pigments were believed to contain the azo group —N=N—, but for approximately 25 years now it has been known that all Hansa yellow pigments (and all other commercial 'azo' pigments) crystallize in the hydrazone form; it would, therefore, be more appropriate to speak of 'hydrazone' pigments.

Pigment Yellow 151 (P.Y. 151, Hostaperm® Yellow H4G) has a greenish yellow shade and is one of the most important pigments for industrial finishes and overcoatings. Owing to its very high light and weather fastness, it is used *e.g.* in automotive refinishes and vehicle paints. P.Y. 151 is heat stable up to 473 K. To our knowledge, only one phase of P.Y. 151 is known. The presence of a carboxylic acid group is rather uncommon in organic pigments, because the introduction of a carboxylic acid group normally increases the solubility of the pigment, *e.g.* in an NaOH solution owing to salt formation. Why the solubility of P.Y. 151 is extremely low in spite of the presence of the carboxylic acid group is not understood, and knowledge of the crystal structure of P.Y. 151 can perhaps help explain this anomaly.

Pigment Yellow 154 (P.Y. 154, Hostaperm® Yellow H3G) is a greenish yellow pigment not as greenish as P.Y. 151. Its good light and weather fastness lead to its usage in industrial paints and coatings, even in automotive finishes. It is also used in printing inks and as a colourant in plastics in which it disperses easily. One of its major features is its bleeding fastness in plasticized PVC. The pigment is heat stable up to 433 K and can be used as an overcoat for steel. The commercially produced phase used to be the only phase known, but as mentioned above, our recrystallization experiments uncovered a DMSO solvate. We will therefore designate the commercial phase as the α phase, the DMSO solvate as the β phase.

Pigment Orange 36 (P.O. 36, Novoperm® Orange HL 70) is a reddish-orange pigment with good light and weather fastness. It is mainly used in industrial lacquers, but also in coatings for off-road applications or agricultural machines because of its good opacity. P.O. 36 is heat stable up to 433 K. Special applications of P.O. 36 are its usage in offset printing and in coatings of hard PVC. Two phases of P.O. 36 are known. The α phase is a brown powder obtained from the commercial synthesis; solvent treatment yields the orange β phase.

Pigment Orange 62 (P.O. 62, Novoperm® Orange H5G 70) is a yellowish orange pigment used mainly in industrial paints, lacquers and coatings and in offset printing. P.O. 62 shows good light and weather fastness. It is thermostable up to 453 K. P.O. 62 has an excellent opacity and thus is often applied as a replacement for lead molybdate pigments. As far as we are aware, only one polymorph is known for P.O. 62.

Pigment Orange 72 (P.O. 72, PV Fast Orange H4GL) is a yellowish orange pigment used for plastic dying, *e.g.* spin dying. P.O. 72 shows a good light fastness. It is heat stable up to temperatures of about 573 K and can be applied in powder lacquers. Owing to its extremely low solubility in all media, there is no bio-availability; the pigment is non-toxic and can be used in food packaging. P.O. 72 exists in four polymorphic forms. Synthesis (azo coupling as shown in Fig. 2) yields the red α phase, which has been known since 1959. By heating a suspension of the α phase in an organic solvent to *ca* 423–473 K the orange β phase is formed; the transformation goes *via* a brown δ phase. It is the bright orange β phase that is industrially produced and sold under trademarks like 'PV Fast Orange H4GL'. Depending on the process parameters in the suspension treatment, a brown γ phase may be formed instead of the orange β phase. Interestingly, the γ phase has been known since 1966, whereas the orange β phase has been produced since 1992.

Pigment Yellow 181 (P.Y. 181, PV Fast Yellow H3R) is a reddish-shaded yellow pigment. It is thermally stable up to 573 K. P.Y. 181 shows excellent light fastness and can hence be used in plastic dying for interior decoration. It is also widely used for colouring laminates, since the shade of P.Y. 181 very closely resembles the colour of real wood. P.Y. 181 has at least ten polymorphs (Hunger & Pesenacker, 1983; Schmidt & Mehltretter, 2006) of which only the β polymorph is produced commercially. The θ phase is not of any commercial interest.

Pigment Yellow 194 (P.Y. 194, Novoperm® Yellow F2G) exhibits a medium yellow shade and a good light fastness. It is heat

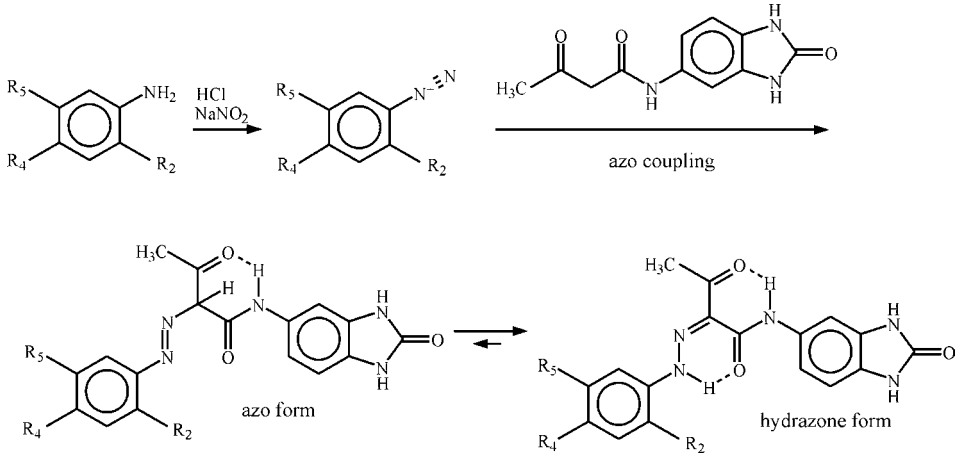

Figure 2
Industrial synthesis of benzimidazolone pigments.

stable up to 473 K. P.Y. 194 is mainly used for industrial coatings and for the colouration of plastics. Owing to its excellent opacity it is used as a replacement for $PbCrO_4$ in coatings. As far as we are aware, only one polymorph is known for P.Y. 194.

The compound with CSD reference code BIRZIL is a development product of the former Hoechst AG and has never been used commercially.

2. Methods and results

2.1. Polymorph screening/recrystallization

For P.O. 72, P.Y. 151, P.Y. 154 and P.Y. 181 we tried to recrystallize the compounds in order to obtain a single-crystal or at least an X-ray powder diffraction pattern of improved quality. In the case of the other pigments (P.O. 36, P.O. 62 and P.Y. 194) the X-ray powder diagrams of the commercial products were sufficient to solve the crystal structures.

For the recrystallization of P.O. 72, P.Y. 151, P.Y. 154 and P.Y. 181 different crystallization methods were used including:

(i) recrystallization from various solvents and solvent mixtures by heating to temperatures of up to 573 K with subsequent slow cooling,

(ii) diffusion of an anti-solvent *via* the gas phase into a solution of the investigated compounds,

(iii) heating the pigments as suspensions in various solvents and solvent mixtures.

Altogether approximately 300 experiments were carried out. For most samples, powder diffraction patterns were recorded and examined for polymorphs.

For P.Y. 151 all samples either showed the same crystalline phase or were amorphous. The sample that showed the best powder diffraction pattern of compound P.Y. 151 was obtained by recrystallization: the pigment was dissolved in boiling DMSO at 462 K; after slow cooling to room temperature the pigment was isolated by filtration and dried at 373 K.

For P.Y. 154 we found two different phases (one of which turned out to be a solvate), but most of the samples were amorphous. Also for this pigment, the sample showing the best powder diffraction pattern was obtained by recrystallization from boiling DMSO (10 mg P.Y. 154 in 1 ml DMSO) with subsequent slow cooling to room temperature. By this procedure the crystallinity of the commercial product could be remarkably improved (see Fig. 3).

During the polymorph screening of P.Y. 154 single crystals were obtained: 10 mg of P.Y. 154 in 4 ml DMSO was heated in a thermostat to 423 K and cooled down to room temperature. After 2 h needles with lengths of up to 2.5 mm had formed, which turned out to be a DMSO solvate of P.Y. 154.

For β-P.Y. 181 the crystallinity was improved in the following way. Approximately 3 g of a sample of β-P.Y. 181 in the form of the commercial product PV Fast Yellow H3R from Clariant (Frankfurt am Main) was suspended in 60 ml of *N*,*N*-dimethylacetamide. The suspension was heated in an oil bath to reflux at 438 K for 8 h, after which the oil bath was switched off and the suspension was left to cool down overnight. The tiny, thin crystals were isolated by filtration, washed with acetone and dried at 333 K. The needles were much too small for a single-crystal structure determination, even on a micro-crystal synchrotron beamline. The material was ground to break the thin needles and thereby reduce the amount of preferred orientation. The θ polymorph was obtained by

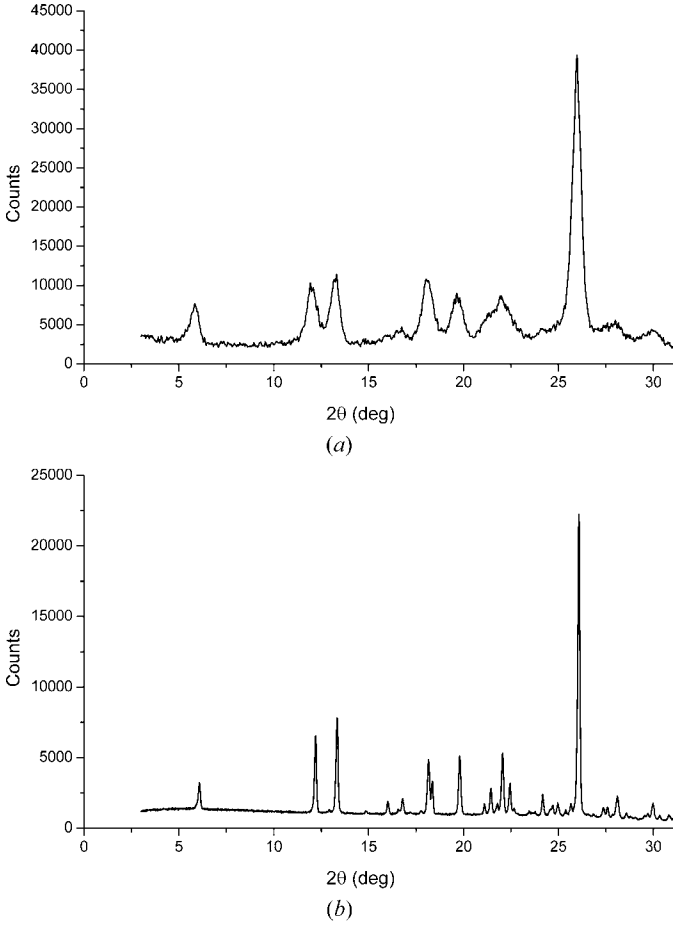

Figure 3
P.Y. 154: powder patterns of the commercial product as purchased (above) and after recrystallization from boiling DMSO (below).

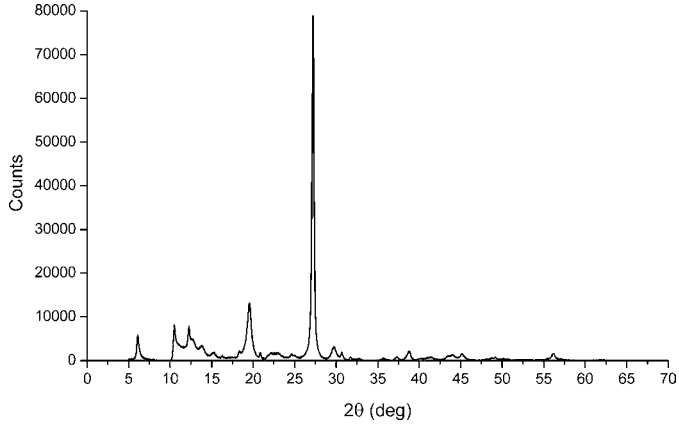

Figure 4
Experimental powder diffraction pattern of β-P.O. 72, after background subtraction.

Table 2
Summary of the crystal structures reported in this paper.

Note that all commercial phases are solvent-free. None of the compounds are hydrates.

Compound	Polymorph	Structure solution
P.O. 36	β (Commercial phase)	Powder
P.O. 62	(Commercial phase)	Powder
P.Y. 151	(Commercial phase)	Powder
P.Y. 154	α (Commercial phase)	Powder
P.Y. 181	β (Commercial phase)	Powder
P.Y. 194	(Commercial phase)	Powder
BIRZIL	(R&D product)	Single crystal†
P.Y. 154	β (DMSO solvate)	Single crystal†
P.Y. 181	θ (DMSO + NMP solvate)	Powder‡

† Structure solution described in §5. ‡ Structure solution described in detail elsewhere (van de Streek, 2009).

completely dissolving 24 parts of P.Y. 181 in the β polymorph in a boiling mixture of 500 parts of DMSO and 500 parts of *N*-methyl-2-pyrrolidone (NMP). Slow cooling to room temperature yields the θ polymorph in powder form (Schmidt & Mehltretter, 2006).

P.O. 72 is completely insoluble in water and any other solvent tried; even at temperatures around 473 K the solubility is less than 1 mg L^{-1}. The compound melts with decomposition at far above 573 K; sublimation is not possible, not even in a high vacuum. All attempts at recrystallization failed. The best X-ray powder diagram ever obtained is shown in Fig. 4; this sample of β-P.O. 72 was obtained by treating a small sample of α-P.O. 72 in *ca* 1 L of a water/isobutanol mixture under pressure at 443 K for 4 h. The α phase is nearly amorphous; the X-ray powder diagram consists of only two broad humps, the sharper one having a full width at half maximum of 2° at $2\theta = 27°$. The powder diagrams of the other phases are somewhat better, but still far from indexable.

Single crystals of BIRZIL were obtained by repeated recrystallizations from dimethylformamide and nitrobenzene. In the end, thin needles with lengths of up to 0.5 mm were formed.

2.2. X-ray powder diffraction

The powders of each compound were measured on a STOE Stadi-P diffractometer with Cu $K\alpha_1$ radiation [curved Ge(111) primary monochromator; λ = 1.5406 Å] in transmission geometry. Each sample was prepared between two Mylar® foils. The samples of the commercial products were measured with a linear position-sensitive detector in the range between 2 and 34° (2θ) with steps of 0.02° (2θ). For the polymorph screening an image-plate position-sensitive detector was used, which allows for more rapid measurements. Recrystallized samples showing the highest degree of crystallinity were additionally carefully measured in a capillary using a linear position-sensitive detector in the range between 2 and 70° (2θ). For all data acquisition the STOE software *WinX*^{POW} was used (STOE & Cie, 2004).

3. Crystal-structure determinations from powder data

For reference, the crystal structures reported in this paper are summarized in Table 2. Atomic coordinates are available in the supplementary material.[1]

3.1. Crystal-structure determinations of β-P.O. 36, P.O. 62, P.Y. 151, α-P.Y. 154, β-P.Y. 181 and P.Y. 194

All six crystal structures were solved by real-space methods from laboratory X-ray powder diffraction data. The crystal structure solution of β-P.Y. 181, which came first chronologically, has been published separately (Pidcock *et al.*, 2007) and was used as a template on which the crystal structure determinations of β-P.O. 36, P.O. 62, P.Y. 151 and α-P.Y. 154 were based; these five crystal structures were solved with *DASH* (David *et al.*, 2006). Because *DASH* resources had been temporarily dedicated to another problem, the crystal structure of P.Y. 194 was solved with *MRIA* (Zlokazov & Chernyshev, 1992). Details are provided in the supplementary material.

3.2. Current limitations of the method

If the crystallinity of the sample is too low, a structure determination from X-ray powder data is no longer possible. This is the case for the β phase of P.O. 72.

The powder patterns of P.O. 72 (see *e.g.* Fig. 4 for the β phase) cannot be indexed: indexing attempts with different programs and conditions resulted in various possible unit cells without it being possible to decide which is the correct one. Pawley fits did not help either. This holds for the β phase as well as for the other crystal phases.

Considerable effort was made to determine the crystal structure of the β phase of P.O. 72 by global lattice-energy minimizations using the program *CRYSCA* (Schmidt & Kalkhof, 1997). For all low-energy structures, X-ray powder patterns were simulated and compared with the experimental powder pattern. However, no good match could be found. Global lattice energy minimizations using the 'Polymorph Predictor' within the *Cerius*^{2} (Accelry, 2003) package gave no better results. The fit between the calculated and the experimental powder patterns could be somewhat improved by taking a low-energy structure from *CRYSCA* and manually shifting the molecular layers against each other, but the simulated X-ray powder pattern (see supplementary material) still deviates considerably from the experimental one and the correct structure remains obscure.

4. Rietveld refinement

Rietveld refinements of β-P.O. 36, P.O. 62, P.Y. 151, α-P.Y. 154, β-P.Y. 181 and P.Y. 194 were carried out with *TOPAS* (Coelho, 2007) using all diffraction data to 1.28, 2.64, 1.28, 1.34, 1.54 and 2.64 Å resolution, respectively. In order to improve the

[1] Supplementary data for this paper are available from the IUCr electronic archives (Reference: OG5035). Services for accessing these data are described at the back of the journal.

Table 3
Structural parameters of the Rietveld refinements of the six pigments.

	β-P.O. 36	P.O. 62	P.Y. 151	α-P.Y. 154	β-P.Y. 181	P.Y. 194
Crystal data						
Chemical formula	$C_{17}H_{13}ClN_6O_5$	$C_{17}H_{14}N_6O_5$	$C_{18}H_{15}N_5O_5$	$C_{18}H_{14}F_3N_5O_3$	$C_{25}H_{21}N_7O_5$	$C_{18}H_{17}N_5O_4$
M_r	416.78	382.34	381.35	405.34	499.49	367.37
Crystal system, space group	Triclinic, $P\bar{1}$	Triclinic, $P\bar{1}$	Triclinic, $P\bar{1}$	Monoclinic, $P2_1/c$	Monoclinic, $P2_1/c$	Monoclinic, $P2_1/c$
Temperature (K)	293	293	293	293	293	293
a, b, c (Å)	8.6533 (7), 9.1170 (6), 11.3831 (6)	7.2689 (8), 10.3176 (14), 12.1761 (15)	5.12970 (14), 9.2292 (3), 17.4094 (6)	14.5848 (5), 8.5448 (2), 13.7794 (4)	22.5510 (8), 4.96366 (13), 21.2815 (6)	14.7172 (16), 5.9852 (5), 20.7919 (13)
α, β, γ (°)	74.717 (2), 81.597 (4), 88.982 (3)	96.462 (6), 95.869 (4), 109.849 (8)	95.857 (2), 95.5056 (17), 91.7980 (13)	90, 96.0670 (19), 90	90, 109.4539 (13), 90	90, 114.818 (4), 90
V (Å^3)	856.78 (10)	843.78 (19)	815.42 (4)	1707.62 (9)	2246.16 (12)	1662.3 (2)
Z	2	2	2	4	4	4
Radiation type	Cu $K\alpha_1$	Cu $K\alpha_1$	Cu $K\alpha_1$	Cu $K\alpha_1$	Cu $K\alpha_1$	Cu $K\alpha_1$
Wavelength of incident radiation (Å)	1.54056	1.54056	1.54056	1.54056	1.54056	1.54056
μ (mm^{-1})	2.41	0.97	0.98	1.15	0.89	0.89
Specimen shape, size (mm)	Cylinder, 10 × 0.7	Flat sheet, 10 × 1.2	Cylinder, 10 × 0.7	Cylinder, 10 × 0.7	Cylinder, 10 × 0.7	Flat sheet, 10 × 1.2
Data collection						
Diffractometer	STOE-Stadi-P	STOE-Stadi-P	STOE-Stadi-P	STOE-Stadi-P	STOE-Stadi-P	STOE-Stadi-P
Specimen mounting	Glass capillary	Flat sample holder	Glass capillary	Glass capillary	Glass capillary	Flat sample holder
Scan method	Step	Step	Step	Step	Step	Step
Data-collection mode	Transmission	Transmission	Transmission	Transmission	Transmission	Transmission
2θ values (°)	$2\theta_{min}$ = 2.00, $2\theta_{max}$ = 75.00, $2\theta_{step}$ = 0.01	$2\theta_{min}$ = 3.00, $2\theta_{max}$ = 34.00, $2\theta_{step}$ = 0.02	$2\theta_{min}$ = 4.00, $2\theta_{max}$ = 74.00, $2\theta_{step}$ = 0.01	$2\theta_{min}$ = 3.00, $2\theta_{max}$ = 70.00, $2\theta_{step}$ = 0.01	$2\theta_{min}$ = 3.00, $2\theta_{max}$ = 60.00, $2\theta_{step}$ = 0.01	$2\theta_{min}$ = 3.00, $2\theta_{max}$ = 34.00, $2\theta_{step}$ = 0.02
Refinement						
R_p, R_{wp}, R_{exp}, χ^2	0.029, 0.039, 0.094, 1.10	0.030, 0.040, 0.055, 1.28	0.015, 0.021, 0.054, 1.37	0.036, 0.047, 0.090, 1.37	0.012, 0.015, 0.036, 1.19	0.029, 0.039, 0.048, 1.32
R'_p, R'_{wp}	0.101, 0.104	0.063, 0.069	0.061, 0.075	0.128, 0.124	0.048, 0.043	0.056, 0.064
Excluded region(s)	None	None	None	None	None	None
No. of data points	9800	1550	7000	6700	5700	1550
No. of parameters	191	190	194	180	224	176
H-atom treatment	Constrained	Constrained	Constrained	Constrained	Constrained	Constrained
No. of restraints	116	118	118	120	162	122

Computer programs used: *WinX^{POW}* (STOE & Cie, 2004), *DASH* (David *et al.*, 2006), *TOPAS* (Coelho, 2007), *Mercury* (Macrae *et al.*, 2008).

stability of the Rietveld refinements, the refinement strategy employed consisted of several stages. An initial Pawley refinement was carried out for each pattern, refining the background, unit-cell parameters, zero-point error, peak-width parameters and peak-asymmetry parameters. To allow the peak profiles to be described as accurately as possible, anisotropic peak broadening was then included in a second Pawley refinement step; for all six patterns, inclusion of anisotropic peak broadening improved the fit noticeably. During a Pawley refinement, all intensities were allowed to refine independently (*i.e.* without reference to a structural model), and the result is therefore the best fit that is theoretically attainable; for all six powder patterns, this fit was excellent, showing virtually no discrepancy between the experimental and the fitted profiles.

The actual Rietveld refinement was then set up. While keeping the profile parameters from the Pawley refinement fixed, the scale parameter, the background parameters and the global isotropic displacement parameter were allowed to refine. The isotropic displacement parameters of the H atoms were constrained at 1.2 times the global isotropic displacement parameter; Cl atoms were given individual isotropic displacement factors. Finally, suitable chemical restraints were added for all bond lengths, valence angles and the planarity of all aromatic systems including the benzimidazolone groups before the atomic coordinates were allowed to refine. The *TOPAS* input files for each step, including all crystallographic constraints and chemical restraints, were generated automatically by the *DASH*-to-*TOPAS* link available in *DASH*3.1, which substantially facilitated the setup of the Rietveld refinements.

It was found that the fit was greatly improved by subsequently refining all peak-shape and unit-cell parameters again, including peak asymmetry and anisotropic broadening values. In the last step of each Rietveld refinement, all parameters were refined simultaneously.

For P.Y. 151 and α-P.Y. 154 the discrepancies between the observed and the calculated profile appeared to systematically depend on the *hkl* indices of the reflections, indicating preferred orientation in the (100) direction for P.Y. 151 and in the (010) direction for α-P.Y. 154. The March–Dollase formula (Dollase, 1986) was used. For β-P.O. 36, P.O. 62, β-P.Y. 181 and P.Y. 194, possible preferred orientation was detected by trying the directions (100), (010) and (001) in succession and judging if the improvement in R_{wp} warranted inclusion of a preferred orientation correction. No additional preferred orientation was found.

For all six patterns, the refinement strategy described here in combination with the excellent set of optimization algorithms implemented in *TOPAS* resulted in fast, smooth and

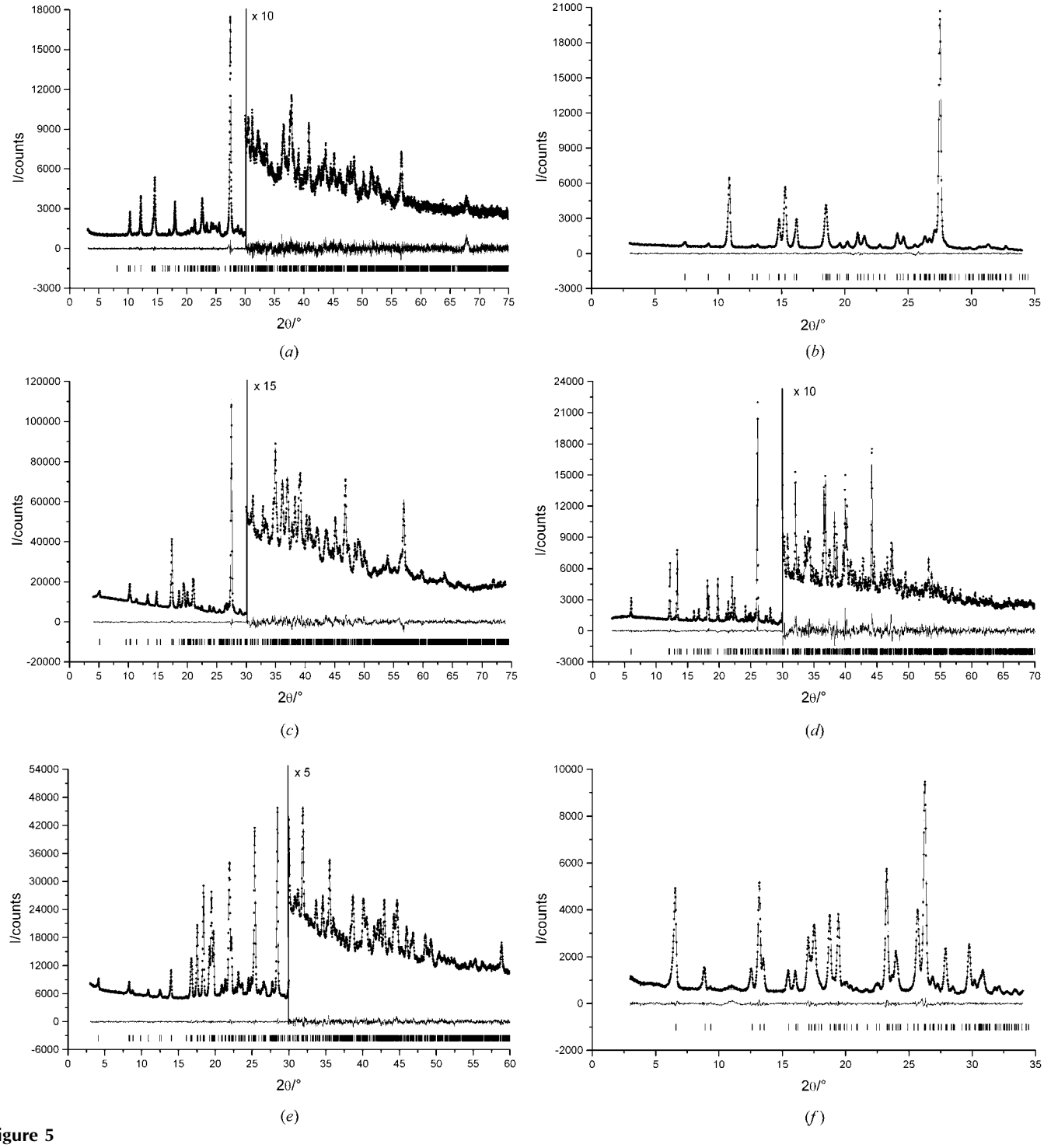

Figure 5
(*a*)–(*f*). Fits of the calculated to the experimental powder diffraction pattern after Rietveld refinement for (a) β-P.O. 36, (*b*) P.O. 62, (*c*) P.Y. 151, (*d*) α-P.Y. 154, (*e*) β-P.Y. 181 and (*f*) P.Y. 194. The experimental data points are shown as points, the calculated patterns as lines and the difference curves as lines under the profiles. Reflection positions are shown as vertical dashes.

Table 4
Structural parameters and figures-of-merit of the remaining two pigments.

	BIRZIL†	β-P.Y. 154‡
Crystal data		
Chemical formula	$C_{18}H_{16}ClN_5O_4$	$C_{18}H_{14}F_3N_5O_3\cdot C_2H_6OS$
M_r	401.81	483.47
Crystal system, space group	Monoclinic, $C2/c$	Triclinic, $P\bar{1}$
Temperature (K)	293	173
a, b, c (Å)	17.126 (2), 5.036 (2), 42.45 (1)	7.5478 (14), 11.941 (2), 13.530 (2)
α, β, γ (°)	90, 97.36 (2), 90	103.996 (14), 101.670 (15), 104.491 (14)
V (Å^3)	3631 (2)	1099.9 (3)
Z	8	2
Radiation type	Cu $K\alpha$	Mo $K\alpha$
μ (mm^{-1})	2.19	0.21
Specimen shape, size	Needle, 0.5 × 0.25 × 0.05	Plate, 0.17 × 0.11 × 0.02
Data collection		
Diffractometer	Nicolet R3 computer-controlled four-circle	STOE IPDS II two-circle
Data collection method	$2\theta/\theta$ scan	ω scan
Absorption correction	None	Multi-scan (based on symmetry-related measurements)
T_{min}	–	0.965
T_{max}	–	0.996
No. of measured, independent and observed reflections	2394, 2303, 971	11 729, 4108, 2452
Criterion for observed reflections	$I > 2\sigma(I)$	$I > 2\sigma(I)$
R_{int}	0.047	0.091
θ_{max} (°)	55.2	25.6
No. and frequency of standard reflections	1 every 40 reflections	None
Refinement		
Refinement on	F^2	F^2
$R[F^2 > 2\sigma(F^2)]$, $wR(F^2)$, S	0.078, 0.198, 0.92	0.065, 0.166, 0.95
No. of reflections	2303	4108
No. of parameters	254	316
H-atom treatment	Mixture of independent and constrained refinement	Mixture of independent and constrained refinement
$(\Delta/\sigma)_{max}$	< 0.0001	< 0.0001
$\Delta\rho_{max}$, $\Delta\rho_{min}$ (e Å^{-3})	0.25, −0.25	0.32, −0.36
Extinction method	*SHELXL*	*SHELXL*
Extinction coefficient	0.00042 (8)	0.023 (4)

Computer programs used: Nicolet software, *X-Area* (STOE & Cie, 2001), *SHELXTL* (Sheldrick, 1981), *SHELXS*97, *SHELXL*97 (Sheldrick, 2008), *XP* in *SHELXTL-Plus* (Sheldrick, 1991). † Non-commercial product, from single crystal data. ‡ DMSO solvate, from single crystal data.

highly stable Rietveld refinements, with excellent agreement between the observed and the calculated powder diffraction patterns. The figures-of-merit are summarized in Table 3; Fig. 5 shows the excellent fits to the experimental patterns. Two unidentified peaks are visible: one in the powder pattern of β-P.O. 36 at 68°2θ, the other in the powder pattern of P.Y. 194 at 11°2θ. These two pigments had not been recrystallized, but the commercial phases had been measured as purchased. The additional peaks may be caused by by-products or additives in the commercial products.

P.Y. 154 contains a trifluoromethyl ($-CF_3$) group; $-CF_3$ groups are often disordered, and hence a disordered model was tried for α-P.Y. 154. The improvement of the fit was small, and within the accuracy of the data it cannot be determined unambiguously if the $-CF_3$ group is disordered or not. Applying Ockham's razor, we decided to include no disorder.

For several of the crystal structures, the positions of some of the H atoms were suboptimal in spite of the restraints applied; therefore, for all crystal structures solved from powder data the positions of all H atoms were optimized, after Rietveld refinement, with the DREIDING/X6 force field (Mayo *et al.*, 1990) keeping the unit-cell parameters and the positions of all non-H atoms fixed.

5. Single-crystal structure analyses

5.1. β-P.Y. 154

Diffraction data for β-P.Y. 154 (the DMSO solvate) were collected as ω scans on a STOE IPDS-II two-circle image plate diffractometer equipped with an Oxford Cryosystems open-flow nitrogen cryostat operating at 173 K. Corrections for absorption were applied by symmetry-related measurements (Blessing, 1995). The crystal structure was solved by direct methods (Sheldrick, 1991) and developed by iterative cycles of least-squares refinement and difference-Fourier synthesis (Sheldrick, 2008). H atoms were placed geometrically and treated in the refinement as part of a riding model, with the exception of:

(i) the methyl hydrogen atoms at C32, which were located from a circular difference-Fourier synthesis and refined as part of a rigid rotating group, and

(ii) the amino H atoms, which were freely refined.

The structure analysis was routine. See Table 4; further details are given in the supplementary material.

5.2. BIRZIL

The crystal structure of BIRZIL was measured and solved in 1981 and the crystal structure solution is described elsewhere in German (Hunger *et al.*, 1982). A crystal of dimensions 0.05 × 0.25 × 0.5 mm^3 was measured on a Nicolet diffractometer at room temperature. Because the crystal was very thin and tended to bend Cu $K\alpha$ radiation was used. The crystal structure was solved with direct methods in *SHELXTL* (Sheldrick, 1981). We redid the refinement using the original

Table 5
Summary of packing features of the nine crystal structures.

	Benzimidazolone hydrogen-bond topology	Second N—H of benzimidazolone	Overall hydrogen-bond topology	Packing
β-P.O. 36	Eight-ring†	Acetyl	Double chain	Layer
P.O. 62	Eight-ring†	NO_2	Chain	Layer
P.Y. 151	Eight-ring with COOH	Acetyl	Chain	Layer
α-P.Y. 154	Eight-ring†	Acetyl	Double chain	Wavy layer
β-P.Y. 181	Helix‡	$CONH_2$	Three-dimensional network	'Three-dimensional'
P.Y. 194	Helix‡	Acetyl	Two-dimensional network	'Three-dimensional'
BIRZIL	Eight-ring†	Acetyl	Double chain	Herringbone
β-P.Y. 154	Eight-ring†	DMSO	Dimers	Layer
θ-P.Y. 181	Eight-ring with $CONH_2$	DMSO	Chain	Wavy layer

† Across the inversion centre. ‡ Along the 2_1 screw axis.

experimental data, but for the present publication we made two changes:

(i) we transformed the unit cell to change β from 105.52° (as given in the original publication) to 97.36° to make β closer to 90°, and

(ii) we re-refined the crystal structure against the original experimental data using F^2 rather than F as used at the time. See Table 4; further details are given in the supplementary material.

6. Discussion of the crystal structures

In all crystal structures of yellow mono-'azo' pigments (be they Hansa or benzimidazolone pigments), two intramolecular hydrogen bonds are formed (see Fig. 1) involving the acetyl, the amide and the hydrazone groups. The benzimidazolone group forms intermolecular hydrogen bonds, sometimes in combination with other functional groups present (like the carboxylic acid group in P.Y. 151). In all nine crystal structures presented here all good hydrogen-bond donors (N—H, COO—H) and acceptors (C═O) are satisfied and the intermolecular hydrogen-bonding patterns in the nine crystal structures have many commonalities. However, there are also marked differences and no two crystal structures in this paper are isostructural. The individual crystal packings will be described per crystal structure, and are summarized in Table 5.

6.1. β-P.O. 36 ($P\bar{1}$)

The benzimidazolone groups of two neighbouring molecules combine across an inversion centre *via* two N—H···O═C hydrogen bonds to form eight-membered rings. The second N—H group of the benzimidazolone fragment forms a hydrogen bond with the acetyl group of another neighbouring molecule. The P.O. 36 molecules build one-dimensional double chains (Fig. 6) which assemble into a layered crystal structure (Fig. 7). The $-NO_2$ group is involved in an intramolecular hydrogen bond only.

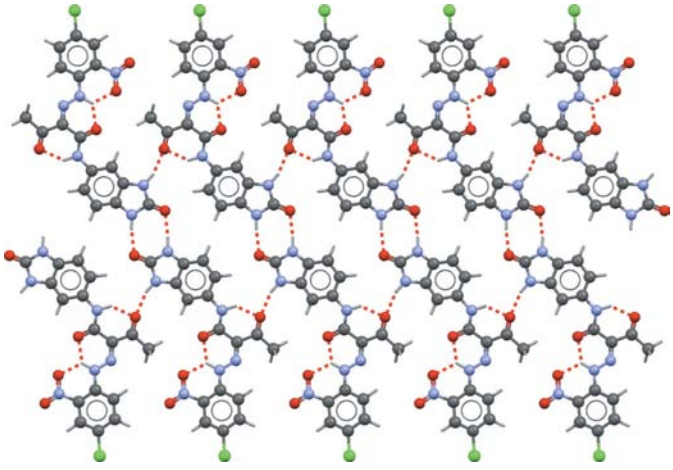

Figure 6
Infinite one-dimensional hydrogen-bonded double chains in β-P.O. 36. The same motif is present in the crystal structures of α-P.Y. 154 and BIRZIL. Hydrogen bonds are shown as dashed red lines.

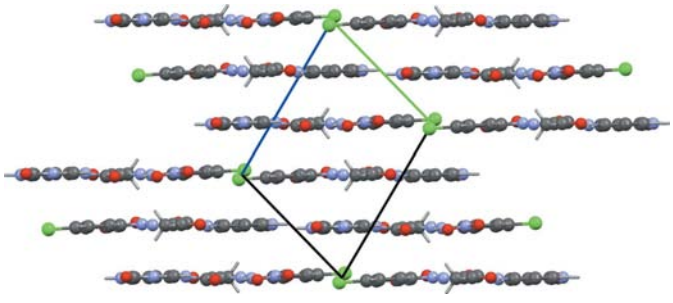

Figure 7
Layer structure of β-P.O. 36. View direction [100].

6.2. P.O. 62 ($P\bar{1}$)

The benzimidazolone groups combine across an inversion centre *via* two N—H···O═C hydrogen bonds to form eight-membered rings. The second N—H group forms a hydrogen bond with the nitro group of a neighbouring molecule, which is slightly surprising because nitro groups are generally not very good hydrogen-bond acceptors. The molecules build chains along the long axis of the molecule (Fig. 8), which assemble into a layered crystal structure.

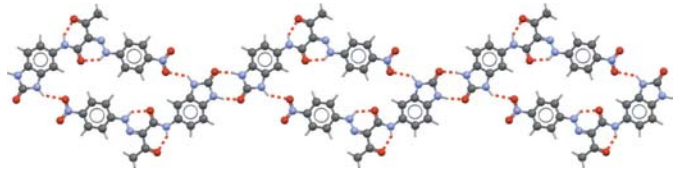

Figure 8
Infinite one-dimensional hydrogen-bonded chains in P.O. 62.

6.3. P.Y. 151 ($P\bar{1}$)

The benzimidazolone group forms an eight-membered hydrogen-bonded ring, not with a second benzimidazolone group but with a COOH group of a neighbouring molecule. The second N—H group forms a hydrogen bond with the acetyl group of the same molecule (Fig. 9). The molecules build chains, which assemble into a layered structure. P.Y. 151 shows an extremely dense packing: whereas in general, organic compounds have a volume increment of *ca* 18 Å^3 per non-H atom (Kempster & Lipson, 1972), this value drops to 14.6 Å^3 for P.Y. 151. The eight-membered hydrogen-bonded ring of the carboxylic acid group with the benzimidazolone group stabilizes the crystal structure considerably. This stabilization would offer an explanation for the insolubility of P.Y. 151, even in NaOH; in other words, the carboxylic acid group no longer behaves like an acid.

Although β-P.O. 36, P.O. 62 and P.Y. 151 crystallize in the same space group ($P\bar{1}$, $Z = 2$) and are all layer structures, their hydrogen-bond topologies are different.

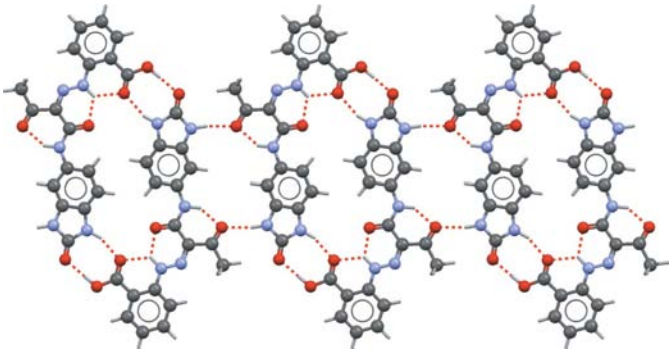

Figure 9
Infinite one-dimensional hydrogen-bonded chains in P.Y. 151. The benzimidazolone hydrogen bonds to the COOH group of a neighbouring molecule.

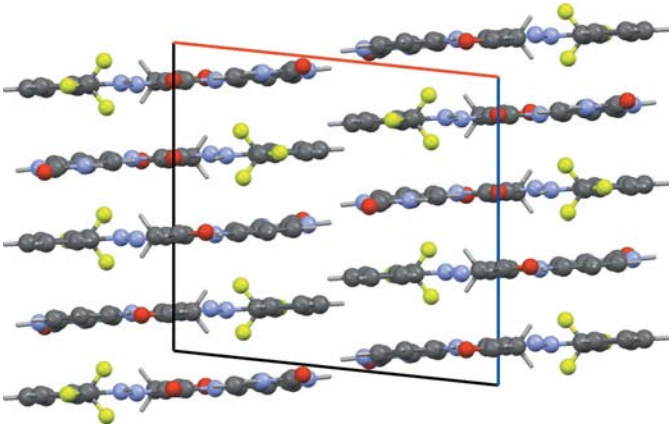

Figure 10
Wavy layer structure of α-P.Y. 154. View direction [010].

6.4. α-P.Y. 154 ($P2_1/c$)

The hydrogen-bond topology is the same as that of β-P.O. 36; α-P.Y. 154, like β-P.O. 36, is a layer structure. The stacking of the chains, however, is different (Fig. 10).

6.5. β-P.Y. 181 ($P2_1/c$)

The benzimidazolone groups do not form an eight-membered ring, but a helix along a 2_1 screw axis. In the same direction, the molecules are connected by two N—H···O=C hydrogen bonds of two of the amide groups (as mentioned, the third amide group, next to the benzimidazolone fragment, is always involved in intramolecular hydrogen bonds). The second N—H group of the benzimidazolone fragment forms a hydrogen bond with the O atom of the $-CONH_2$ group. For more details, see Pidcock *et al.* (2007).

6.6. P.Y. 194 ($P2_1/c$)

The benzimidazolone groups form a helix along a 2_1 screw axis (Fig. 11). The other N—H group forms a hydrogen bond with the acetyl group of a neighbouring molecule, resulting in a two-dimensional hydrogen-bond network.

6.7. BIRZIL ($C2/c$)

The hydrogen-bond topology is the same as those in β-P.O. 36 and α-P.Y. 154, but the double chains are arranged in a herringbone pattern (Fig. 12) instead of layers.

6.8. β-P.Y. 154 ($P\bar{1}$; DMSO solvate)

The benzimidazolone groups combine across an inversion centre *via* two N—H···O=C hydrogen bonds to form eight-membered rings. The second N—H group forms a hydrogen bond with the O atom of the DMSO molecule. This results in dimers consisting of two P.Y. 154 molecules with adjacent DMSO molecules.

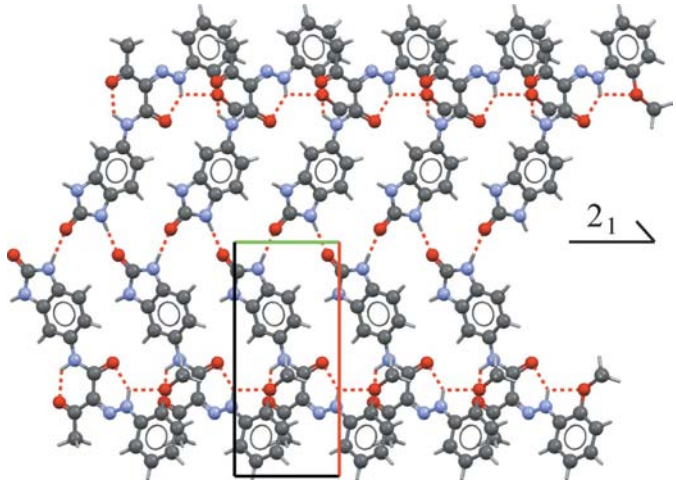

Figure 11
The helix along a 2_1 screw axis, formed by hydrogen-bonded benzimidazolone groups in the crystal structure of P.Y. 194. View direction [001].

6.9. θ-P.Y. 181 ($P\bar{1}$; solvate with DMSO and NMP)

The hydrogen-bonding network in the θ-P.Y. 181 solvate is completely different from all the other crystal structures and involves intermolecular hydrogen bonds to the DMSO and the NMP solvent molecules, resulting in a chain topology.

6.10. Comparison of the molecular conformations

The molecular geometries of the nine experimentally determined crystal structures are compared in Fig. 13. In β-P.O. 36, P.O. 62, P.Y. 151, α-P.Y. 154, θ-P.Y. 181 (the DMSO+NMP solvate) and BIRZIL, the molecules are planar. In β-P.O. 36 and in P.O. 62, the $-NO_2$ group is coplanar with the adjacent phenyl ring and therefore with the rest of the molecule. In contrast, the molecules in β-P.Y. 181 are not exactly planar: the $-CO-NH-$ group between the two phenyl rings as well as the terminal $-CO-NH_2$ group are twisted out of the plane to form hydrogen bonds. In β-P.Y. 154 (the DMSO solvate) the molecules are slightly twisted: the angle between the planes through the two phenyl rings is 14.3°. In P.Y. 194 the molecule is bent in the centre, the angle between the planes through the two phenyl rings is 18.6°.

As can be seen from Fig. 13, the benzimidazolone group can have either of two distinct orientations, differing by a rotation of 180°. In the crystal structures of P.Y. 151 and P.Y. 194 the benzimidazolone groups adopt one orientation; in all other crystal structures they adopt the other orientation.

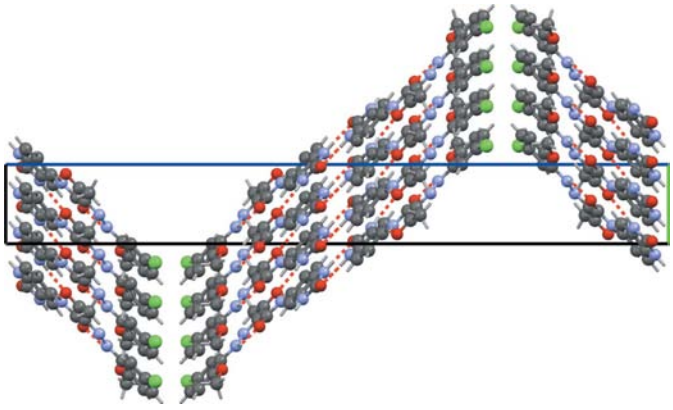

Figure 12
Herringbone packing in the crystal structure of BIRZIL. View direction [100].

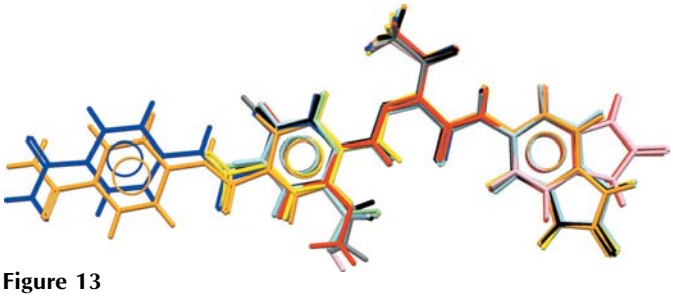

Figure 13
Comparison of the molecular geometries in the nine experimentally determined hydrazone benzimidazolone crystal structures. Light green: β-P.O. 36, yellow: P.O. 62, pink: P.Y. 151, light blue: α-P.Y. 154, orange: β-P.Y. 181, red: P.Y. 194, grey: BIRZIL, black: β-P.Y. 154 (DMSO solvate), blue: θ-P.Y. 181 (solvate with DMSO and NMP).

7. Conclusion

If powder diffraction data of reasonable quality are available, modern day computers and software allow routine crystal structure solution of moderately flexible molecules even from laboratory powder diffraction data. This enables crystal structure solution for materials with extremely poor solubility, in this case organic pigments.

The crystal structures of the six industrial phases described in this paper show high degrees of intermolecular hydrogen bonding, with all good hydrogen-bond donors and acceptors being satisfied. In contrast, intermolecular hydrogen bonding is absent in the more soluble Hansa pigments. The extremely low solubility of the mono-'azo'-benzimidazolone pigments is therefore easily explained as being due to the extensive intermolecular hydrogen bonding.

In spite of the variety of compounds and polymorphs, no two phases solved thus far have turned out to be isostructural, and we obtained ten different crystal structures. Interestingly, the six industrially produced pigments exhibit five different hydrogen-bond topologies. Apparently, the outstanding fastness properties of the benzimidazolone pigments are not caused by one specific hydrogen-bonding pattern or crystal structure type; the packing may vary as long as an efficient molecular packing with good intermolecular hydrogen bonds and low lattice energies are formed. For industrial pigments, several additional criteria like clear shades and availability of raw materials play a role, of course.

The crystal structures of α-P.O. 36, as well as of the α-, γ- and δ phases of P.O. 72 remain obscure, because the crystallinities of these samples are too low and the X-ray powder data only contain between two and 16 broad peaks, and do not allow crystal structure determination. The quality of the unindexable diffraction pattern of β-P.O. 72, with approximately 30 broad peaks, is already beyond the limit for structure solution from X-ray powder data for a molecule of this complexity.

Frank Becker (Clariant) is gratefully acknowledged for the recrystallization experiments on P.O. 72. Dr Lothar Fink and Edith Alig (Frankfurt University) are gratefully acknowledged for the collection of several of the powder diffraction patterns.

References

Accelrys (2003). *Cerius2*, Version 4.9. Accelrys Ltd, Cambridge Science Park, Cambridge, England.
Allen, F. H. (2002). *Acta Cryst.* B**58**, 380–388.
Blessing, R. H. (1995). *Acta Cryst.* A**51**, 33–38.
Coelho, A. A. (2007). *TOPAS Academic 4.1*, http://members.optusnet.com.au/~alancoelho/.

David, W. I. F., Shankland, K., van de Streek, J., Pidcock, E., Motherwell, W. D. S. & Cole, J. C. (2006). *J. Appl. Cryst.* **39**, 910–915.
Dietz, E. & Schilling, K. (1963). *Water-Insoluble Azo Pigments*, US-Patent 3109842.
Dollase, W. A. (1986). *J. Appl. Cryst.* **19**, 267–272.
Herbst, W. & Hunger, K. (2004). *Industrial Organic Pigments: Production, Properties, Applications.* Weinheim: Wiley-VCH.
Hunger, K., Paulus, E. F. & Weber, D. (1982). *Farbe Lack*, **88**, 453–458.
Hunger, K. & Pesenacker, M. (1983). Monoazoverbindungen der Acetoacetylaminobenzimidazolonreihe, Verfahren zu ihrer Herstellung und ihre Verwendung, European Patent EP 0 010 273 B1.
Kempster, C. J. E. & Lipson, H. (1972). *Acta Cryst.* B**28**, 3674.
Macrae, C. F., Bruno, I. J., Chisholm, J. A., Edgington, P. R., McCabe, P., Pidcock, E., Rodriguez-Monge, L., Taylor, R., van de Streek, J. & Wood, P. A. (2008). *J. Appl. Cryst.* **41**, 466–470.
Mayo, S. L., Olafson, B. D. & Goddard III, W. A. (1990). *J. Phys. Chem.* **94**, 8897–8909.
Metz, H. J. & Morgenroth, F. (2002). *High Performance Pigments*, edited by H. M. Smith, pp. 135–158. Weinheim, Germany: Verlag Wiley-VCH.
Paulus, E. F. (1982). *Z. Kristallogr.* **160**, 235–243.
Pidcock, E., van de Streek, J. & Schmidt, M. U. (2007). *Z. Kristallogr.* **222**, 713–717.
Schilling, K. & Dietz, E. (1964). *Water-Insoluble Benzimidazolinone Monoazo Dyes.* US-Patent 3124565.
Schmidt, M. U. & Kalkhof, H. (1997). *CRYSCA*. Frankfurt am Main, Germany.
Schmidt, M. U. & Mehltretter, G. (2006). *Novel Crystalline Modifications of C.I. Pigment Yellow 181 and Associated Production Method.* World Patent Application WO 2006005408.
Sheldrick, G. M. (1981). *SHELXTL*. University of Göttingen, Germany.
Sheldrick, G. M. (1991). *SHELXTL-Plus*, Release 4.1. Siemens Analytical X-ray Instruments Inc., Madison, Wisconsin, USA.
Sheldrick, G. M. (2008). *Acta Cryst.* A**64**, 112–122.
STOE & Cie (2001). *X-Area*. STOE & Cie, Darmstadt, Germany.
STOE & Cie (2004). *WinX^{POW}*. STOE & Cie, Darmstadt, Germany.
Streek, J. van de (2009). In preparation.
Zlokazov, V. B. & Chernyshev, V. V. (1992). *J. Appl. Cryst.* **25**, 447–451.